Immunol Genet J, Vol. 8, No. 1, 2025, pp.100-110 DOI: https://doi.org/10.18502/igj.v8i1.17995

Original Article

Evaluation of Tumor Immune Microenvironment Changes in Response to Different Radiotherapy Regimens in a CT26 Tumor Model

Masoumeh Alimohammadi[1], Haniyeh Ghaffari Nazari[2], Reza Alimohammadi[3], Mohsen Bakhshandeh[4], Seyed Amir Jalali[3*], Nima Rezaei[1,5,6*]

[1] *Department of Immunology, School of Medicine, Tehran University of Medical Sciences, Tehran, Iran*
[2] *Department of Immunology, School of Medicine, Mashhad University of Medical Sciences, Mashhad, Iran*
[3] *Department of Immunology, School of Medicine, Shahid Beheshti University of Medical Sciences, Tehran, Iran*
[4] *Department of Radiology Technology, Allied Medical Faculty, Shahid Beheshti University of Medical Sciences, Tehran, Iran*
[5] *Research Center for Immunodeficiencies, Children's Medical Center Hospital, Tehran University of Medical Sciences, Tehran, Iran*
[6] *Network of Immunity in Infection, Malignancy and Autoimmunity (NIIMA), Universal Scientific Education and Research Network (USERN), Tehran, Iran*

Received: 14 September 2024; Accepted: 27 January 2025

Abstract

Background: Radiotherapy (RT) is vital in cancer treatment, inducing tumor cell death and anti-tumor immunity. However, it can also enhance immunosuppressive factors like CD47 and PD-L1. While RT-immunotherapy combinations show promise, optimal strategies remain unclear. This study examines the impact of different RT regimens on the tumor immune microenvironment (TME) to guide more effective treatment approaches.

Methods: We treated CT26 tumor-bearing mice with three distinct RT regimens under the same biological equivalent dose (BED).

Results: We observed that the frequency of both tumor-infiltrating $CD4^+$ and $CD8^+$ cells were increased after ablative and hypo RT, although single high dose exposure in an ablative scheme led to a greater extent of $CD8^+$ cells infiltration and increased the expression of IFNγ in those cells. While conventional RT enhanced the recruitment of myeloid-derived suppressor cells (MDSCs) into tumors, the Ablative and hypo schemes induced regulatory T cells (Tregs) enrichment. The two hypofractionated regimens enhanced the expression of CD47 as well as the PD-1/PD-L1 axis, although PD-1 and its ligand (PD-L1) expression were temporarily induced by conventional RT on tumor-infiltrating lymphocytes and tumor cells, respectively.

Conclusion: The results suggest targeting the recruitment of MDSC and Treg are, respectively, crucial for therapeutic efficacy of conventional and hypofractionated RT regimens. Furthermore, anti-PD-1/PD-L1 and anti-CD47 treatments are necessary to improve the anti-tumor response from the hypofractionated schemes.

Keywords: Immune Response; Immune Checkpoint Inhibitor; CT26 Colon Cancer; Radiotherapy

***Corresponding Authors:** Seyed Amir Jalali
Department of Immunology, School of Medicine, Shahid Beheshti University of Medical Sciences, Tehran, Iran
E-mail: jalalia@sbmu.ac.ir

Nima Rezaei, MD, PhD
Research Center for Immunodeficiencies, Children's Medical Center Hospital, Tehran University of Medical Sciences, Tehran, Iran
E-mail: rezaei_nima@tums.ac.ir

How to cite this article
Alimohammadi M, Ghaffari Nazari H, Alimohammadi R, Bakhshandeh M, Jalali SA, Rezaei M. Evaluation of Tumor Immune Microenvironment Changes in Response to Different Radiotherapy Regimens in a CT26 Tumor Model. Immunol Genet J, 2025; 8(1): 100-110. DOI: https://doi.org/10.18502/igj.v8i1.17995

Introduction

Radiotherapy (RT) is commonly used in the treatment of cancer and it has remained a major treatment approach in controlling a broad variety of solid malignancies for many years (1) with approximately 60% of cancer patients receiving it as curative or alleviative care. Despite the main mechanism of RT action, which is the non-repairable genomic DNA damage, resulting in mitotic catastrophe, apoptotic death of tumor cell, and tumor shrinkage (2), RT can also stimulate systemic anti-tumor immune responses (3).

Mechanistically, RT triggers immunologic cell death with the release of specific damage-associated molecular patterns (DAMP) from affected tumor cells, which in turn lead to the maturation of dendritic cells and activation of their cytosolic DNA sensing cGAS/STING pathway and type 1 interferon induction. These together improve cross-presentation of tumor antigens and the following antigen-specific responses by CD8+ T-cell (4). Many studies indicate that, in addition to immunostimulation, RT may also exert opposite effects or augment the already immunosuppressed tumor immune microenvironment (TME) through increasing suppressive immune cell infiltration as well as induction of various immune-suppressive factors like CD47 and PD-L1 (5).

As a means to reduce these inhibitory barriers and enhance RT-induced antitumor effects, the association of RT with immunotherapy modalities has been proven to be effective in different studies over recent years (6,7). Furthermore, multiple clinical studies are being conducted to assess these combinations, but nevertheless, the optimal combinations capable of controlling tumor growth remain to be defined. Given that different radiation doses and fractionation protocols distinctly affect the tumor phenotypes as well as the host immune system (8,9), investigating TME changes following them may provide rationales for selecting immunotherapy targets which are fitting best to each RT scheme.

The purpose of this study was to evaluate the impact of three different RT protocols with the equivalent biological equivalent dose (BED) on immune cell components as well as the expression of immune checkpoint molecules which are targets of modulatory monoclonal antibodies (10).

Material and Methods

Cell Culture and Reagents

CT26 murine colon cancer cells (Pasteur Institute of Iran, Tehran, Iran) were maintained in RPMI-1640 media (Gibco, US), supplemented with 10% fetal bovine serum (FBS) (Gibco, US) (37 °C, 5% carbon dioxide and 95% humidity) and were cultured to limited passage before implantation. PerCP labeled Rat anti-mouse CD4 antibody, APC labeled anti-mouse CD 45 antibody, PE-labeled Rat anti-mouse CD8a antibody, NIR Zombie die (for live/Dead discrimination), PE-labeled Rat anti-mouse CD25 antibody, Alexa-flour labeled Rat anti-mouse Foxp3 antibody, Alexa Fluor® 488 labeled anti-mouse CD47, PE labeled anti-mouse CD274 (B7-H1, PD-L1) Antibody, PerCP labeled anti-mouse/human CD11b Antibody, PerCP labeled anti-mouse/human CD11b Antibody, Alexa Fluor® 488 labeled anti-mouse CD80 Antibody, PE labeled anti-mouse CD206 (MMR).

Antibody, as well as appropriate isotype control antibodies, Cell Activation Cocktail (with Brefeldin A) and a True-Nuclear™ transcription factor buffer set, all were obtained from Biolegend (CA, San Diego). Collagenase type I was obtained from Gibco (NY, USA). Dnase type I was obtained from Roche (USA). The rest of reagents were chemical grade.

Mice and Tumor Induction

Four to six weeks old female BALB/c mice were obtained from the Pasteur Institute of Iran. Animals were kept properly under controlled conditions throughout the experiment. To induce tumors, anesthetized Mice were inoculated subcutaneously with a unit injection of 1 × 106 CT26 tumor cells in 100 µl of ice-cold PBS into their right flank as described previously. When there were signs of pain and considerable necrosis, or the total tumor volume measured greater than 1500 mm3, we euthanized them by Carbon dioxide (CO2) inhalation under Isoflurane 2.5% anesthesia.

Treatments

On day 19 after tumor induction (when tumors were at least 250 mm^3), we assigned the animals to 4 distinct therapy groups in a way that achieved

equal averages of tumor volume across the groups, including an unirradiated control group (Control), a high-dose ablative group ("Ablt") being given a single dose of 16 Gy on day 19, a hypofraction group ("Hypo") receiving 2 fractions of 10 Gy with 10 days interval and a conventional group ("Conv") receiving 10 doses of 3 Gy commencing from day 19 to day 31. We performed these 3 radiation schemes in a way giving an identical total biologically effective dose (BED). For BED calculation, we applied the linear quadratic (LQ) formula (BED = D (1 + d / [α/β]), where "D" and "d" are, respectively, total dose and dose per fraction, and the α/β ratio is about 10 to 12 Gy, for most solid tumors and acutely responding normal tissues.

According to the LQ model, radiotherapy effect doses for different fractionation schemes can be estimated. Based on α/β= 10 ratio for tumor area, our RT regimens had a BED of 40 Gy. To anesthetize the mice prior to and throughout the irradiation, they were intraperitoneally given 100 mg/kg of ketamine 10% and 12.5 mg/kg of Xylazine 2% (Alfasan, Sofia, Bulgaria). A clinical linear accelerator (Elekta synergy linear accelerator, Stockholm, SE) with 6 MV energy X-ray photons was applied to irradiate the mice. All efforts were made to reduce the mice's pain and anxiety. We restrained the mice in an altered 50 ml falcon tube with two holes, one on the bottom for breathing and one on the body for exposing the tumor area to radiation, while the remaining of the body was kept out of the field of radiation. Excluding the radiation field, we covered every part of the body with 9 cm of lead plate in order to provide protection during radiation. The field of 3×3 cm2 with 5-mm margins was tangentially irradiated with a dose rate of 3.5 Gy/min. A 1.5 cm super flab bolus material was located over the tumor area, while the interval from the source to the skin was 100 cm.

Treatment Effects; Survival Factors

The treatment efficacy was assessed by determining the survival percent and measuring a tumor growth deceleration parameter which is the time needed for the treated tumor to reach a volume of 1500 mm^3. For each group, 5 mice were used to evaluate tumor growth and survival, whereas the 6 others were used for flowcytometry analysis. The tumor sizes were recorded using calipers along two orthogonal axes three times per week, and the tumor volume (TV) was estimated according to the formulation: TV = (a × b × b)/2, where a and b are respectively, the longest and shortest diameter of the tumor. We calculated the survival time from the day of tumor induction until the day of the protocol endpoint (TV ≥1500).

Tumor Preparation and Flowcytometry

As a way of evaluating tumor microenvironment changes following different RT schemes, flow cytometry was used for tumor analysis. At two different therapy time points, including 3 and 7 days post the final session for each scheme (while the total dose was delivered), three mice from each group were euthanatized, and their tumors were dissected **(Figure 1a)**. The excised tumors were mechanically chopped into small pieces and then enzymatically dissociated using a cocktail of collagenase 2 mg/ml and Dnase 10 IU/ml in RPMI medium at 37˚C. After 90 minutes of digestion, to obtain single-cell suspensions, the cells were filtered through a 70 μm cell strainer (BD Falcon, USA).

We suspended the final pellet, collected by centrifugation (300g, 10 min), in flowcytometry staining buffer (phosphate-buffered saline with 5% FBS) and stained 106 cells with fluorochrome conjugated antibodies according to the manufacturer's recommendation. For IFNγ intracellular staining, cells were incubated with the PMA/Ionomycin (cell activation cocktail) for four hours in the presence of Brefeldin A to restimulate T cells prior staining. Then, all stained samples were washed and acquired on FACS Lyrics flowcytometer (BD Bioscience, USA) and data were analyzed using FlowJo.10 software.

Using specific antibodies mentioned above, live cells were gated (by NIR Zombie die), and the phenotype of cell population infiltrates within the tumor microenvironment, as well as the expression of some checkpoint molecules, was examined in order to analyze the effect of different RT schemes. All gating strategies included doublet cell exclusion gates (FSC-A/FSC-H and SSC-A/SSC-H) and a dead cell exclusion gate (negative with Fixable Viability Dye, APC-Cy7-zombie dye). Gating strategy for $CD8^+$, $CD4^+$, Tregs, MD-

SCs, M1 MQ, M2 MQ and CT26 tumor cells are, respectively, mentioned below: $CD45^+$, SSC^{low}, $CD8a^+$ / $CD45^+$, SSC^{low}, $CD4^+$, $FoxP3^-$ / $CD45^+$, SSC^{low}, $CD4^+$, $FoxP3^+$ / $CD45^+$, $CD11b^+$, $Gr1^+$ / $CD45^+$, CD11b+, $CD80^+$ / $CD45^+$, $CD11b^+$, $CD206^+$ / $CD45^-$, FSC ^{hi}.

Ethics Approval

All animal studies were approved by the Institutional Ethical Committee and Research Advisory Committee of Tehran University of Medical Sciences with code ethic number IR.TUMS.MEDICINE.REC.1399.768. The study is reported following ARRIVE guidelines. All methods were performed by the relevant guidelines and regulations.

Statistics and Graphical Representation

Using Prism, version 8.0 (GraphPad SoftwareTM, USA), we performed Statistical analysis and produced all figures. The results were expressed as mean ± standard error of the mean (SEM). For two-group and multiple-group comparisons, the t-test and the one-way ANOVA test were used, respectively. Differences in survival were analyzed by the Log-rank Mantel-Cox test. A p-value less than 0.05 ($*p$ <.05, $**p$ <.01, $***p$<.001) was assumed to be statistically significant.

Results

Survival and Tumor Growth Profile

Initially, we sought to investigate whether different RT fractionation schedules induce different tumor control. We chose 3 regimens with the same BED, including 10*3Gy for the conventional fractionated RT regimen, 2*10Gy for the hypofractionated RT regimen, and 1*16Gy for the ablative high-dose RT regimen **(Figure 1a)**. At day 19 post CT26 tumor induction in Balbc mice, the corresponding RT regimen for each group was started. As shown in **Figure 1b,c**, all three different regimens slowed down tumor growth and significantly enhanced the survival of mice compared to the control group, while there was no significant difference between them. Moreover, they failed to significantly differ in the average time required to reach 1500 mm3 of tumor volume, although it was longest with the ablative group (p= 0.0038) **(Figure 1d)**, which demonstrates that an ablative regimen can elicit a much better tumor control.

Comparison of Immune Cell Infiltrates into Tumor Microenvironment after Different RT Schemes

$CD4^+$ and $CD8^+$ Cells Accumulated Following Ablative and Hypofractionated RT

As it is apparent in **Figure 2a**, seven days after the final fraction of the Ablative regimen and Hypofraction RT regimen, there was a considerable increase in the frequency of $CD4^+$ cells ($1.81 \times 10^6 \pm 1.76 \times 10^5$ and $1.94 \times 10^6 \pm 2.76 \times 10^5$ respectively) compared to the control group, to the fractionated method and also to their counterpart for previous time point. Seven days after 16 Gy exposure in ablative group, $CD8^+$ cell number was highest ($2.42 \times 10^6 \pm 2.82 \times 10^5$) compared to control group ($8.24 \times 10^5 \pm 2.01 \times 10^5$) ($p < 0.0001$), the same regimen group at day 3 ($1 \times 10^6 \pm 2.87 \times 10^5$) ($p = 0.0002$) and the day 7 conventional group ($1.32 \times 10^6 \pm 3.15 \times 10^5$) ($p = 0.0022$). Furthermore, in this time point, the Hypofraction RT also induced a significant accumulation of $CD8^+$ cells ($1.72 \times 10^6 \pm 3.17 \times 10^5$) compared to the day 3 group ($9.57 \times 10^5 \pm 1.28 \times 10^5$) ($p$=0.034) and control group (p=0.01) **(Figure 2b)**. Accordingly, after 7 days, the less RT was fractionated, the more CD8 numbers were recorded. We also investigated the impact of RT on immunosuppressive $CD4^+$ cells and found variations similar to those seen in $CD4^+$ cells **(Figure 2c)**.

Compared to the control group ($4.83 \times 10^4 \pm 1.55 \times 10^4$), a significant accumulation of Treg cells was observed seven days after Hypofraction ($1.07 \times 10^5 \pm 1 \times 10^4$) ($p$= 0.001) and Ablative regimen ($8.53 \times 10^4 \pm 1 \times 10^4$) ($p$= 0.041). Furthermore, the increase in Treg cell numbers in day 7 Hypofraction group was also significant compared to its day3 counterpart group ($6.63 \times 10^4 \pm 1.71 \times 10^4$) ($p$= 0.02) and the day 7 conventional group ($5.53 \times 10^4 \pm 9.07 \times 10^3$) ($p$= 0.003). To evaluate the functionality of tumor-infiltrating $CD8^+$ T cells, their IFNγ expression was assessed on day 7 after irradiation, represented in **Figure 2d**. The proportion of $CD8^+$ T cells secreting IFNγ was highest with ablative regimen (26.7%) compared to conventional (16.3%) (p=0.004) and hypo

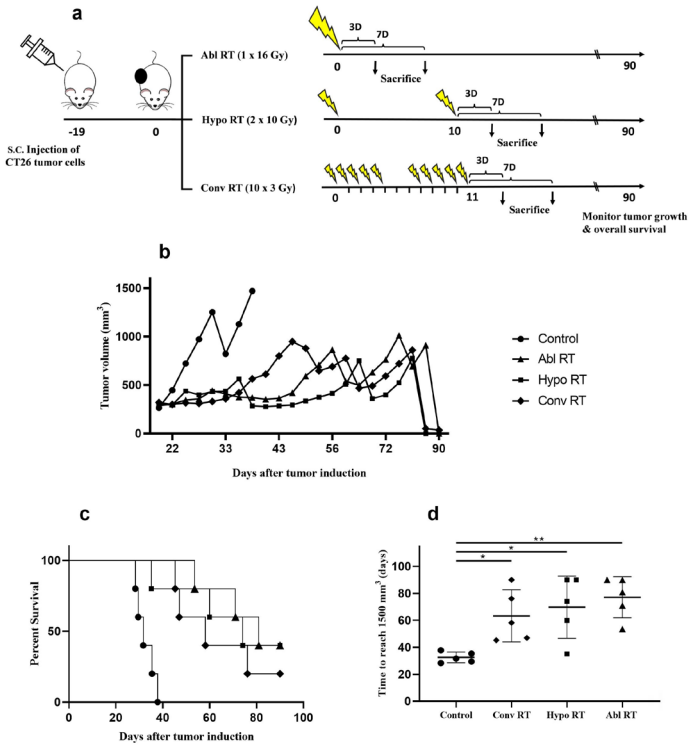

Figure 1. Evaluating the tumor growth profile of CT26 tumors receiving different fractionation regimens of radiotherapy. (a) Schematic of the experimental timeline. The tumor model was established by injecting 106 CT26 cells into the right hind legs of BALBC/c mice, after which when tumors reached around 250 mm3 in volume, day 19 post tumor inoculation, mice were randomly assigned to an unirradiated control group (Control) and 3 treatment groups illustrated in different symbols. On days 3 and 7, after delivery of the last fraction of each RT scheme, three mice from each group were euthanized while the rest were monitored for tumor growth and anti-tumor efficacy. (b) Growth of irradiated tumors after the indicated treatments. Each data point represents the mean of 5 mice per group, error bars are not shown for the purposes of clarity. (c) Survival curves for the indicated radiotherapy treatment groups with log-rank tests were used to compare groups. (d) Times to reach 1500 mm3 expressed in means with standard deviations

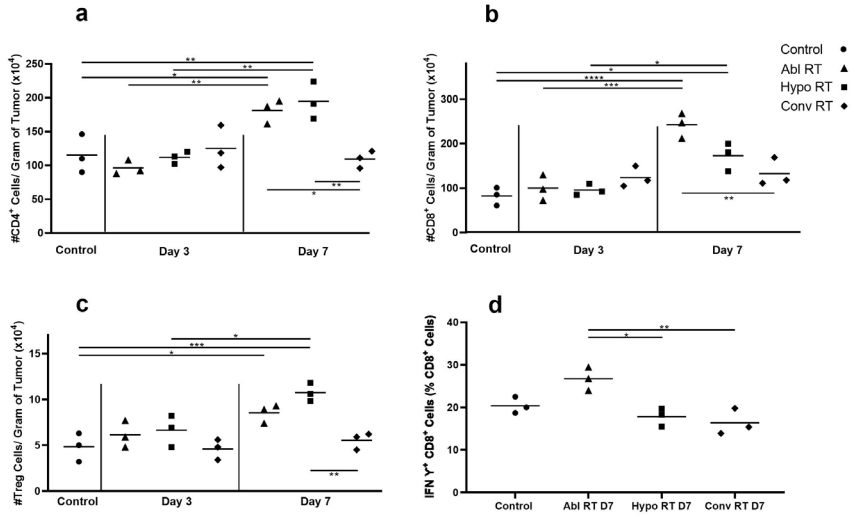

Figure 2. Analysis of lymphoid cell infiltrates into tumor microenvironment following different RT schemes. On days 3 and 7, after delivery of the last fraction of each RT scheme, three mice from each group were euthanized. Tumors were harvested and subjected to flow cytometry analysis. The frequency of $CD4^+$ cells (a), $CD8^+$ cells (b), and $CD4^+$ $CD25^{+-}$ $Foxp3^+$ Treg cells (c) is illustrated per gram of tumor. The IFN-γ expression is shown as the percentage of $CD8^+$ cells in tumor (d).

(17.8%) (p=0.01).

Myeloid Cells Changed Differentially by Different Schemes: Ablative Regimen Increased M1 Macrophages While the Fractionated Conventional RT Increased MDSCs

In **Figure 3**, we represent the variations of tumor-infiltrating myeloid cells. The conventional RT increased the number of MDSC per gram of tumor at day 7 ($3.93 \times 10^6 \pm 2.26 \times 10^5$), which was highest compared to all other groups. In contrast to conventional regimen findings, the infiltration of MDSCs was significantly decreased 7 days post the last dose of ablative and Hypofraction groups compared to the infiltration level of the same groups at day 3 **(Figure 3a)**.

Compared to the control tumor ($7.50\times 10^5\pm 1.97 \times 10^5$), the infiltration of M1 MQ cells was significantly increased at day 7 after tumors were irradiated by a single high dose regimen ($1.31\times 10^6 \pm 2.01 \times 10^5$) ($p$=0.038). As shown in **Figure 3b**, this difference was much higher in comparison to day 3 ($3.81\times 10^5\pm 1.03\times 10^5$) ($p$=0.0006), when there was a decrease in M1 MQ number, although not significant. The number of M2 MQ at none of the time points was not significantly influenced by radiation, regardless of the RT protocol we used **(Figure 3c)**. The M1/M2 ratio was highest on day 7 after the ablative regimen (4.45± 1.3), and its changes were similar to those observed in the M1 MQ number **(Figure 3d)**.

Check-Point Analysis in the Tumor Microenvironment after RT

To provide further context to the RT-mediated alteration in the TME, we also assessed the expression of some check-point molecules using flowcytometry. Assessing the alterations of PD-1 and its ligand (PD-L1) expression revealed that RT affects their expression depending on radiation dose and the time post-dose.

We observed that the expression of PD-L1 on tumor cells at day 3 was upregulated by all three schemes compared to control (p=0.0315, 0.0003, and 0.0031 for Abl, Hypo, and Conv, respectively). While this effect was timely restricted and declined by 7 days after conventional radiation, it remained significantly elevated by the two others. The expression of PD-L1 on MDSCs was also changed in a similar manner, which represents a likely effect of TME condition **(Figure 4a,b)**.

Figure 4c shows that the PD-1 expression level on $CD4^+$ cells at day 3 was not notably affected by RT, regardless of the regimen used. At the next kinetic time point, day 7, the ablative and hypo fractionated regimen enhanced PD-1 expression on both $CD4^+$ (p=0.031 0.01425 and p= 0.0008, respectively) and $CD8^+$ cells (p <0.0001 and p= 0.0043, respectively) when compared with its expression on infiltrating T cells in control tumor **(Figure 4c,d)**. Indeed, ablative RT delivered as 16 Gy in a single fraction induced stronger PD-1 upregulation in $CD8^+$ cells, while this effect was more conspicuous after hypo-fractionated RT in $CD4^+$ cells.

Conventional RT enhanced PD-1 expression level on $CD8^+$ cells at day 3, in comparison to data of the control group; p= 0.0035), which was a transient effect and didn't remain significant at day 7, which is similar to what we observed in variations of PD-L1 expression after this regimen.

In addition to the PD-1/PD-L1 axis, we also assessed the impact of the aforementioned RT protocols on the expression of two other immune checkpoints, including CTLA4 and CD47. Radiotherapy, regardless of our assessment time point and the irradiation protocols that we used, did not influence the expression of CTLA4 on CT26 tumor cells **(Figure 4e)**.

Tumors that received the mono, as well as the hypo fractionated RT, showed enhanced expression of CD47. This increase was only significant at day 7 (p= 0.0327 and p= 0.0099 for Abl and Hypo RT, respectively, when compared with CD47 expression on control tumor), in which the CD47 upregulation was even more pronounced following hypo fractionated RT **(Figure 4f)**.

Discussion

This original work represents the variation of tumor immune microenvironment induced by different fractionation protocols. Currently, several trials are testing the association of RT with other treatments, aiming to maximize the chances of favorable outcomes for patients. There are, however, some unaddressed issues pertinent to the optimal Radiotherapy delivery approaches, as well as the best-matched immunotherapy and its scheduling (11). It is, therefore, of great significance to discover how different fractionation and

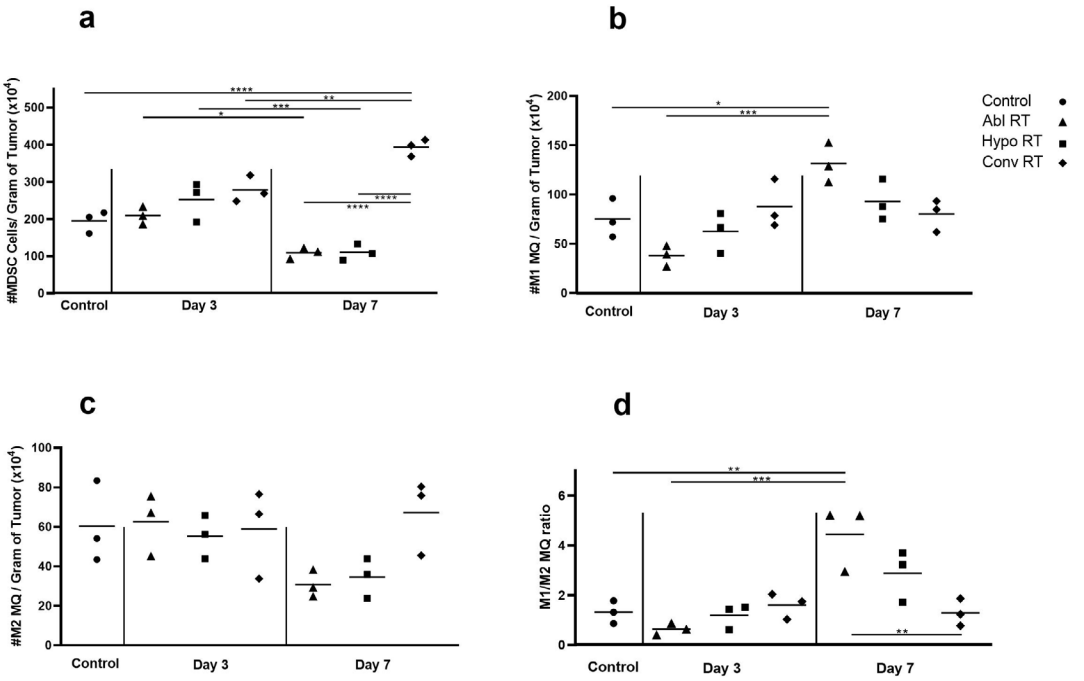

Figure 3. Analysis of myeloid cell infiltrates into tumor microenvironment following different RT schemes. On days 3 and 7, after delivery of the last fraction of each RT scheme, three mice from each group were euthanized. Tumors were harvested and subjected to flow cytometry analysis. The frequency of myeloid-derived suppressor cells (MDSC) (a), M1 (b) and M2 (c) macrophages is illustrated per gram of tumor. The M1/M2 ratio (d) was calculated by dividing the M1 MQ numbers (CD11b+ CD80+) by the M2 MQ numbers (CD11b+ CD206+).

dosing schemes affect the TME in the hope of designing more effective radiotherapy combinations. In most of the studies comparing different radiation schemes, the BED was not equal (12,13). We, therefore, used the BEDs of 40 gray for our three schemes as we did in our last study (14), and our flow cytometric analysis showed different RT protocols modulate the immune microenvironment differently despite the same BED.

Our study revealed a predominantly $CD4^+$ and $CD8^+$ cells infiltrate 7 days after the mono and hypo-fractionated radiation while treatment with conventional radiotherapy, conversely, couldn't significantly affect this population. This is consistent with the findings of Grapin *et al.* (15) who suggested that repeated exposure to radiation may result in lymphopenia, which explains the lack of lymphoid response following the conventional method. In addition, adding a fractionated regimen (10 * 3 Gy) after an ablative single dose regimen (30 Gy) resulted in diminishing the potent $CD8^+$ T-cell response triggered by the single dose itself (16). Based on these results, it has been found that conventional fractionation regimens may negatively affect the TME by killing the infiltrating lymphocytes, possibly leading to tumor relapse.

In agreement with previous high-dose irradiation studies (12,17), we found an increase in the frequency of $IFN\gamma^+$ $CD8^+$ cells infiltrating into the tumor following ablative radiation. However, the hypo-fractionated and conventional regimens failed to induce the IFNγ expression in the tumor milieu. These results did not contradict those of a study (18) in a mouse melanoma model showing that a single dose of 15 Gy radiation leads to accumulation of IFNγ secreting cells and augmented $CD8^+$ T cell-mediated cell lysis in comparison to fractionated RT.

Although several studies have reported an increase in Tregs after radiation (19-21), in our study, only hypo and ablative regimens showed such an effect while the conventional one maintained low Treg numbers. This fractional dose dependency of radiation effects on Tregs has been observed in a recent study (15) in contrast to their two hypo-fractionated schemes, fractionating the radiation did not impact Treg cell proportion sig-

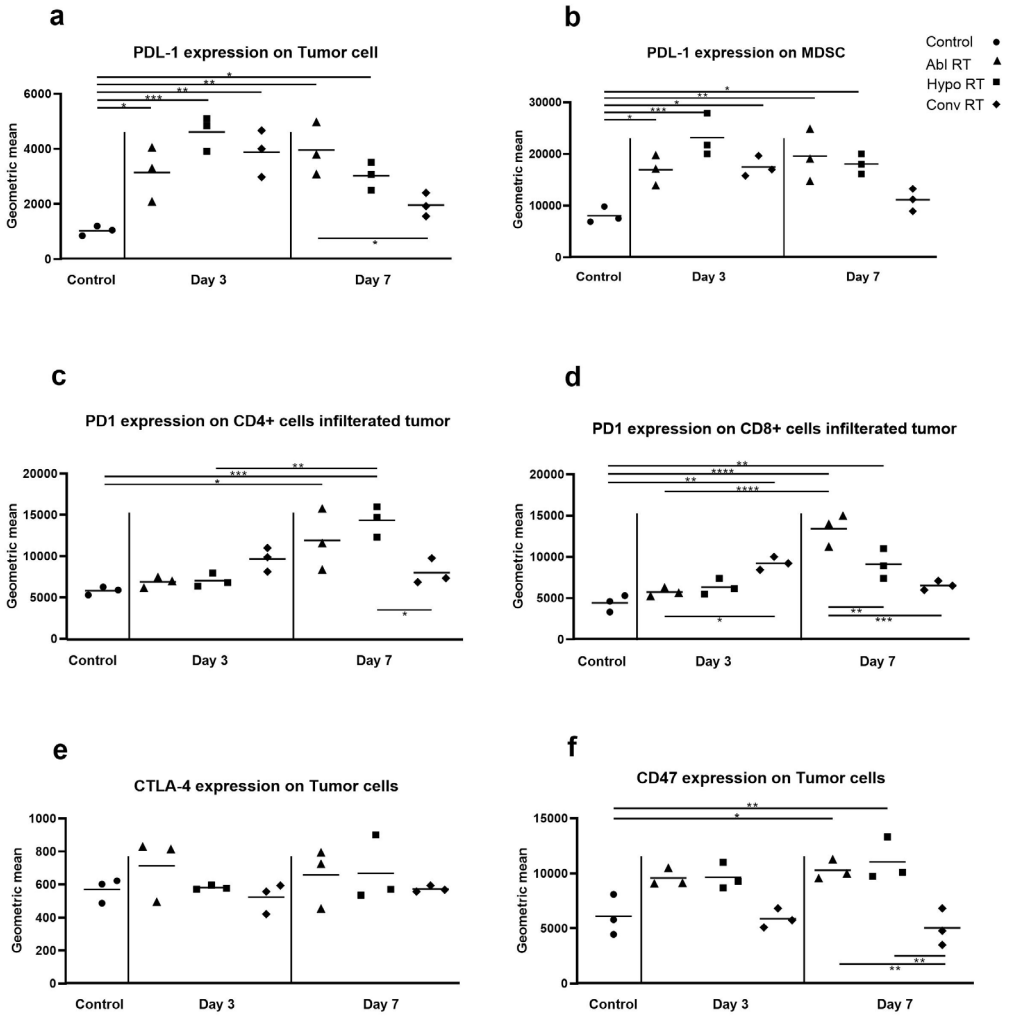

Figure 4. The expression evaluation of immune checkpoint molecules following different RT schemes. The established subcutaneous CT26 tumors were irradiated with different fractionation regimens as described in Figure 1. Mice were euthanized on days 3 and 7 after the final dose. The tumor tissues were collected, and the expression of PD-L1 on tumor cells(a) and on MDSCs (b), PD1 on the infiltrating lymphocyte (c, d), CTLA4 (e), and CD47 (f) on tumor cells were assessed.

nificantly, which is in agreement with our finding. Inhibitory Treg cells are considered to be a strong contributor to the immunosuppressive TME; thus, by integrating Treg-targeting therapies into hypo and ablative radiation therapy, the $CD8^{+}$/Treg ratio will be increased, resulting in exploiting the radiation-induced effector T cell infiltration in TME.

MDSCs are immature myeloid cells with robust immunosuppressive functions and can be both boosted and restricted by RT depending on dose-fractionation protocols. It has been shown that conventional fractionated RT (CFRT) induces the accumulation of MDSC (22,23), while treatment with ablative hypofractionated RT (AHFRT) (24) and a single high-dose scheme (16) led to MDSC removal. Similar results were observed in the present study in which the conventional regimen caused a predominantly myeloid response by increasing MDSCs while the other regimens decreased their frequency instead. Therefore, it would be critical to combine MDSC depletion strategies with conventional RT to overcome this suppressive phenotype.

The RT can skew TAMs to a pro-inflammatory phenotype, M1 MQ, which provokes an anti-tumor immunity. In our study, this effect required high-dose radiation, and it wasn't observed in tumors given several smaller radiation doses. On the contrary, it has been concluded from the

literature that high doses of irradiation (defined as doses higher than 10 Gy) reprogram macrophages toward the M2 phenotype, which have pro-tumoral and pro-metastatic functions, while M1-like macrophages can be promoted by doses from 1 to 10 Gy (25). This inconsistency may be explained by the fact that the results found in the literature came from different cell lines or tumor models, seeing that our MQ findings were compatible with those found in a recently published study using the same CT26 tumor (15).

We further found that, different RT protocols differently affect the expression of some checkpoint molecules, as well. Analysis of CT-26 tumors showed that the expression of PD-1/PD-L1 axis is enhanced in the TME by hypo and ablative regimens. The higher PD-L1 expression on MDSCs and tumor cells was observed at the early day 3 time point post-RT and it remained significantly high at day 7. This data can be supported by others' findings (26,27), despite using different cell lines. One study reported the PD-L1 upregulation in TME three days after a single 12-Gy dose of IR (26) and another demonstrated increased PD-L1 expression within both primary and secondary tumors at day 7 post a single fraction of 15 Gy (27).

Furthermore, recent data, from a similar tumor model (15) demonstrated that hypo fractionated schemes increase the tumoral PD-L1 expression at one week post dose which is another support for our data. In this study, the upregulated tumoral PD-L1 at day 7 was also observed by fractionated RT, which is inconsistent to our conventional RT data, where it diminished by day 7. One possible explanation for these discrepancies is that our analysis time point was at 7 days after the final dose of RT, while it was at 7 days after the first dose in their study. Another possibility is the different conventionally fractionated regimens, which have an extended pattern, delivered in 12 fractions of 2 GY in the mentioned study, while our conventional RT was performed in ten fractions of 3 Gy and caused temporal increases in expression of PD-1 and its ligand observed at day 3 post final dose of radiation. Similarly, Dovedi *et al.* (28) found that a conventionally low dose fractionated RT scheme (5x2Gy) leads to the highest expression of PD-L1 on tumor cells and $CD11b^{+}$ $GR1^{hi}$ MDSCs at day 3 post-RT while it diminishes significantly during a week. In this study, an improved tumor control was only observed with anti-PD-L1 mAb therapy administered simultaneously with conventionally fractionated RT, but not with the sequentially mode.

In our experiments, besides increasing the presence of PDL1 in the TME, the ablative and hypo fractionated schemes enhanced PD-1 expression on both intra tumoral CD4 and CD8 expressing cells 7 days post-treatment, which probably made the tumors more amenable to treatment with Anti-PD-1/PD-L1 blockade combined with the mentioned regimens. Although PD-1 expression is commonly associated with the exhaustion of T cells, but it has been shown that exhausted T cells are characterized by sustained co-expression of several suppressing receptors (29). Therefore, T cells with RT-induced PD1 upregulation are not necessarily exhausted, as it has been confirmed in the findings of Park *et al.* in which $PD\text{-}1^{+}$ $CD8^{+}$ T cells produced IFNγ at irradiated tumors as well as the non-irradiated areas, suggesting they are effector within the tumors. In this study, the authors affirmed in a melanoma model that a single SABR fraction of 15 Gy heightened the expression of PD-1 by $CD11a^{hi}$ $CD8^{+}$ T cells after 7 days which is similar to our data on ablative RT.

Although many radiotherapy combination approaches to date have targeted the PD-1/PD-L1 and CTLA-4 axis, inhibiting other negative checkpoint proteins like CD47 (an innate immune checkpoint) can also be applied for using an immunosuppressive TME into an opportunity for treatment. CD47 as a signal of self, is an anti-phagocytic marker in tumor cells and its blocking increases macrophage-mediated clearance of tumor cells (30). It has been shown that radiation can affect the expression of CD47, although the opposite results are reported in two studies (31,32). Our study is the first report comparing the effect of three different RT schemes on CD47 expression and demonstrated that this effect varies with the fractionation schedule. Paradoxically, one recent study showed that both the single or fractionated RT, irrespective of the schedule, are able to elevate the expression of CD47 in a number of radiation-refractory breast cancer cell lines after 16 hours (31). In the current study, we observed that the ablative and hypo fractionated radiation increased the level of tumoral CD47,

which is in an apparent conflict with the findings of another study by Vermeer *et al.* Indeed, these authors in human papillomavirus-positive cancer demonstrated that CD47 is reduced dose-dependently by radiation (leading to immune-mediated clearance of tumor cells), although this decrease was not permanent, and CD47 expression was restored over time (32). Both of these contradictions with our study could probably be due to the differences in cell lines as well as the time point of analysis. Thus, our CD47 data provide a rationale for adding CD47 inhibitory strategies to these hypo-fractionated RT regimens.

Conclusion

In this study, despite no substantial differences in survival between regimens, our three radiation regimens differently changed the composition of intra-tumoral immune cells as well as the TME immune checkpoints. Collectively, based on our results, conventional RT may need to be combined with MDSC-targeting therapy strategies, while specific targeting of tumor-infiltrating Treg cells seems to be a more rational combination choice in association with ablative and hypo RT. Our results suggest that adding both anti-PD-L1 and anti-CD47 treatments to the ablative regimen, as well as the hypo RT, is necessary for making the most of radiation-induced anti-tumor immunity. Although anti-PD-L1 immunotherapy may also serve as a good fit for conventional RT if it is added at the right time paralleled with PD-1/PD-L1 axis upregulation. Further research is required to validate the most appropriate combination approach with each RT scheme.

Conflict of Interest

The authors declare no competing interests.

Acknowledgments

The work was funded by a grant from the Tehran University of Medical Sciences (grant number 98-01-30-41391).

References

1. Orth M, Lauber K, Niyazi M, Friedl AA, Li M, Maihöfer C, et al. Radiation and Environmental Biophysics. 2014;53:1-29.
2. Liauw SL, Connell PP, Weichselbaum RR. New paradigms and future challenges in radiation oncology: an update of biological targets and technology. Sci Transl Med. 2013;5(173):173sr172.
3. Formenti SC, Demaria S. Systemic effects of local radiotherapy. Lancet Oncol. 2009;10(7):718.
4. Arnold KM, Flynn NJ, Rubinsteyn A, Wang Y, Spratt DE, Morgan TM, et al. The impact of radiation on the tumor microenvironment: effect of dose and fractionation schedules. Cancer Growth Metastasis. 2018;11:1179064418761639.
5. Wang Y, Deng W, Li N, Neri S, Sharma A, Jiang W, et al. Combining immunotherapy and radiotherapy for cancer treatment: current challenges and future directions. Front Pharmacol. 2018;9:185.
6. Bernstein MB, Krishnan S, Hodge JW, Chang JY. Immunotherapy and stereotactic ablative radiotherapy (ISABR): a curative approach? Nat Rev Clin Oncol. 2016;13(8):516-24.
7. Deloch L, Fuchs J, Rückert M, Fietkau R, Frey B, Gaipl US, et al. Modern radiotherapy concepts and the impact of radiation on immune activation. Front Oncol. 2016;6:141.
8. Gunderson AJ, Young KH. Exploring optimal sequencing of radiation and immunotherapy combinations. Adv Radiat Oncol. 2018;3:494.
9. Aliru ML, Schoenhals JE, Venkatesulu BP, Anderson CC, Barsoumian HB, Younes AI, et al. Radiation therapy and immunotherapy: what is the optimal timing or sequencing? Immunotherapy. 2018;10(4):299-316.
10. Kiaie SH, Ghorbani A, Safari M, Rezaei-Tavirani M, Firoozpour L, Taheri-Anganeh M, et al. Immune checkpoints in targeted-immunotherapy of pancreatic cancer: new hope for clinical development. Acta Pharm Sin B. 2021;11(4):1083-97.
11. Romano E, Honeychurch J, Illidge TM. Radiotherapy-immunotherapy combination: how will we bridge the gap between pre-clinical promise and effective clinical delivery? Cancers (Basel). 2021;13(3):457.
12. Schaue D, Ratikan JA, Iwamoto KS, McBride WH. Maximizing tumor immunity with fractionated radiation. Int J Radiat Oncol Biol Phys. 2012;83(4):1306-10.
13. Vanpouille-Box C, Alard A, Aryankalayil MJ, Sarfraz Y, Diamond JM, Schneider RJ, et al. DNA exonuclease Trex1 regulates radiotherapy-induced tumour immunogenicity. Nat Commun. 2017;8:15618.
14. Ghaffari-Nazari H, Heidari S, Nazari M, Khabazian H, Namdar A, Baradaran B, et al. Radiation dose and schedule influence the abscopal effect in a bilateral murine CT26 tumor model. Int Immunopharmacol. 2022;108:108737.
15. Grapin M, Richard C, Limagne E, Boidot R, Mor-

gand V, Bertaut A, et al. Optimized fractionated radiotherapy with anti-PD-L1 and anti-TIGIT: a promising new combination. J Immunother Cancer. 2019;7:160.
16. Filatenkov A, Baker J, Mueller AM, Kenkel J, Ahn GO, Dutt S, et al. Ablative tumor radiation can change the tumor immune cell microenvironment to induce durable complete remissions. Clin Cancer Res. 2015;21(16):3727-39.
17. Lee Y, Auh SL, Wang Y, Burnette B, Wang Y, Meng Y, et al. Therapeutic effects of ablative radiation on local tumor require CD8+ T cells: changing strategies for cancer treatment. Blood. 2009;114(3):589-95.
18. Lugade AA, Sorensen EW, Gerber SA, Moran JP, Frelinger JG, Lord EM, et al. Local radiation therapy of B16 melanoma tumors increases the generation of tumor antigen-specific effector cells that traffic to the tumor. J Immunol. 2005;174(12):7516-23.
19. Wirsdörfer F, Jendrossek V, Rödel F, Fietkau R, Gaipl US, Frey B, et al. Thorax irradiation triggers a local and systemic accumulation of immunosuppressive CD4+ FoxP3+ regulatory T cells. Radiat Oncol. 2014;9:98.
20. Muroyama Y, Nirschl TR, Kochel CM, Harris-Bookman S, McDaniel MM, Bruno TC, et al. Stereotactic radiotherapy increases functionally suppressive regulatory T cells in the tumor microenvironment. Cancer Immunol Res. 2017;5(11):992-1004.
21. Price JG, Idoyaga J, Salmon H, Hogstad B, Bigarella CL, Ghaffari S, et al. CDKN1A regulates Langerhans cell survival and promotes Treg cell generation upon exposure to ionizing irradiation. Nat Immunol. 2015;16(10):1060-8.
22. Ostrand-Rosenberg S, Horn LA, Ciavattone NG. Radiotherapy both promotes and inhibits myeloid-derived suppressor cell function: novel strategies for preventing the tumor-protective effects of radiotherapy. Front Oncol. 2019;9:215.
23. van Meir H, Nout RA, Welters MJ, Loof NM, de Kam ML, van Ham JJ, et al. Impact of (chemo) radiotherapy on immune cell composition and function in cervical cancer patients. Oncoimmunology. 2017;6(2):e1267095.
24. Lan J, Lu Y, Wang X, Jin X, Wu Y, He L, et al. Targeting myeloid-derived suppressor cells and programmed death ligand 1 confers therapeutic advantage of ablative hypofractionated radiation therapy compared with conventional fractionated radiation therapy. Int J Radiat Oncol Biol Phys. 2018;101(1):74-87.
25. Genard G, Lucas S, Michiels C. Reprogramming of tumor-associated macrophages with anticancer therapies: radiotherapy versus chemo- and immunotherapies. Front Immunol. 2017;8:828.
26. Deng L, Liang H, Xu M, Yang X, Burnette B, Arina A, et al. Irradiation and anti-PD-L1 treatment synergistically promote antitumor immunity in mice. J Clin Invest. 2014;124(2):687-695.
27. Park SS, Dong H, Liu X, Harrington SM, Krco CJ, Grams MP, et al. PD-1 restrains radiotherapy-induced abscopal effect. Cancer Immunol Res. 2015;3(6):610-619.
28. Dovedi SJ, Adlard AL, Lipowska-Bhalla G, McKenna C, Jones S, Cheadle EJ, et al. Acquired resistance to fractionated radiotherapy can be overcome by concurrent PD-L1 blockade. Cancer Res. 2014;74(19):5458-5468.
29. Wherry EJ, Kurachi M. Molecular and cellular insights into T cell exhaustion. Nat Rev Immunol. 2015;15(8):486-499.
30. Lu Q, Sun EE, Klein RS, Flanagan KM. Potential new cancer immunotherapy: anti-CD47-SIRPα antibodies. Onco Targets Ther. 2020;13:9323-9323.
31. Candas-Green D, Xie B, Huang J, Fan M, Wang A, Menaa C, et al. Dual blockade of CD47 and HER2 eliminates radioresistant breast cancer cells. Nat Commun. 2020;11:4591.
32. Vermeer DW, Spanos WC, Vermeer PD, Bruns AM, Lee KM, Lee JH, et al. Radiation-induced loss of cell surface CD47 enhances immune-mediated clearance of human papillomavirus-positive cancer. Int J Cancer. 2013;133(1):120-129.